Advanced Composites and Hybrid Materials (2022) 5:1460–1476
https://doi.org/10.1007/s42114-021-00356-4

ORIGINAL RESEARCH

Effects of rare earth neodymium (Nd) and heat treatment on anti-corrosion behaviors of the AZ80 magnesium alloy

Minjie Liang[1] · Huan Liu[1] · Cun Wu[1] · Yida Li[1] · Zhanhu Guo[2] · Vignesh Murugadoss[3]

Received: 1 June 2021 / Revised: 12 September 2021 / Accepted: 27 September 2021 / Published online: 18 January 2022

Abstract

The effect of rare earth neodymium (Nd) and heat treatment on the corrosion resistance of AZ80-xNd ($x = 0$, 0.5, and 1.0 wt.%) magnesium alloys was investigated. Compared to the as-cast AZ80 magnesium alloy, new rod-shaped Al_3Nd phase and block-shaped Al_2Nd phase were observed in AZ80-Nd alloy. Moreover, β-$Mg_{17}Al_{12}$ phase becomes fine and discontinuous. The reduction of the β-$Mg_{17}Al_{12}$ phase and the formation of the Al-Nd binary phase significantly reduced the corrosion rate of the AZ80-Nd alloy by suppressing micro-galvanic corrosion of the alloy. However, with increase in the the wt.% of Nd, the Al-Nd binary phase content increases, and the grain size become coarser, thereby lowering the corrosion resistance of the alloy. Therefore, the as-cast 0.5% Nd alloy with fine grain structure has a good corrosion resistance. After the solution treatment, the β-$Mg_{17}Al_{12}$ phase and part of the Al-Nd binary phase were dissolved in the magnesium matrix, which facilitates the occurrence of corrosion. Therefore, the corrosion rate of solution treated alloys is higher than that of the as-cast alloys. After aging treatment, the β-$Mg_{17}Al_{12}$ phase and Al-Nd binary phase are re-precipitated along the grain boundaries and within the grains, respectively. The fine and uniformly distributed β-$Mg_{17}Al_{12}$ phase, rod-shaped Al_3Nd phase and block-shaped Al_2Nd phase effectively improve the corrosion resistance of the alloy, so that the corrosion rate of the aged alloy is the lowest. The electrochemical and immersion measurements revealed that the aged AZ80-0.5%Nd alloy had the best corrosion resistance.

Keywords AZ80 magnesium alloy · Anticorrosion behavior · Nd element · Heat treatment

1 Introduction

As a commercialized magnesium alloy [1–4], Mg–Al-Zn magnesium alloy has been widely used in automotive industry [5, 6], especially in engine cylinder block, inner frame of door, vehicle wheel, due to its low density, high specific strength, good shock absorption capabilities, and recyclability [7–10]. In addition, the rapid development of 5G communication has stimulated further requirements for lightweight materials, leading to a rapid growth in its applications. However, the applications of magnesium alloys were still limited due to its poor corrosion resistance [11–13]. For automotive products, they are mainly exposed to the atmospheric environment; therefore, it is necessary to improve their corrosion resistance.

Alloying is an important way to improve the corrosion resistance of magnesium alloys. Rare earth elements (such as Nd, Y, Zr, Ce) are regarded as one of the best candidates for alloying, vitally affect their purification of melt effect, and refine the grains to reduce the corrosion tendency effect etc. Nd is an effective element to improve the corrosion resistance of magnesium alloys. For example, Zhang et al. [14] demonstrated that Nd can refine the grain size, and the lowest corrosion rate (3.95 mg/cm^2/day) occurs at 0.9% Nd content; further studies showed that higher potential of $Al_{11}Nd_3$ favor reducing

✉ Minjie Liang
499134232@qq.com

✉ Zhanhu Guo
zguo10@utk.edu

✉ Vignesh Murugadoss
vigneshmurugadoss15@gmail.com

[1] School of Materials Science and Engineering, North University of China, Taiyuan 030051, China

[2] Integrated Composites Laboratory (ICL), Department of Chemical and Bimolecular Engineering, University of Tennessee, Knoxville, TN 37996, USA

[3] Advanced Materials Division, Engineered Multifunctional Composites (EMC) Nanotech LLC, Knoxville, TN 37934, USA

the interfacial corrosion of α-Mg/NaCl solution effectively. Zhang et al. [15] found that the proper Nd addition is beneficial for the formation of the long period stacked ordered (LPSO) phase and $Mg_{12}Nd$ phase. The LPSO phase and $Mg_{12}Nd$ phase act as the cathode and the α-Mg phase as the anode in alloys, and with the addition of 0.5% Nd, the corrosion rate has the lowest value of 0.52 mm/year.

Heat treatment is another way to improve the corrosion resistance of magnesium alloys. For example, Yang et al. [16] reported that the corrosion rate of the alloy treated with T6 was lower than that of the as-cast alloy. Wang et al. [17] found that heat treatment changed the corrosion resistance of AZ91D alloy in the simulated body fluid (SBF) effectively; the configuration and size of the β-$Mg_{17}Al_{12}$ phase were the main factors affecting the corrosion rate of the alloy and acted as a barrier against corrosion. However, the effects of Nd element and heat treatment on the corrosion properties for AZ80 magnesium alloy are still open questions.

As a lightweight material, AZ80 magnesium alloy has great potential in automotive applications, but many researchers are committed to improving its mechanical properties [18–20]; as an external component, it is easy to corrode under the influence of external environment. Therefore, it is necessary to study the corrosion behavior and mechanism of AZ80 magnesium alloy. Few earlier works have studied the effect of single addition of Nd on the corrosion resistance of AZ80 magnesium alloy, and the effect of Nd on the heat-treated AZ80 magnesium alloy is even less. But, the corrosion mechanism of Nd on AZ80 magnesium alloy in medium has seldom been proposed. Therefore, the aim of this work is to investigate the effect of Nd element and heat treatment on the corrosion resistance of AZ80 alloy.

2 Experimental

2.1 Materials

The chemical compositions of the AZ80-xNd (x=0, 0.5, and 1.0 wt.%) magnesium alloys are shown in Table 1.

2.2 Heat treatment process

Based on previous research, the solution treatment process of AZ80-xNd (x=0, 0.5, and 1.0 wt.%) alloys was performed at 420 °C for 12h, and the aging treatment was carried out at 175 °C for 28h of AZ80 alloy, 175 °C for 32h of AZ80-0.5% Nd, and 175 °C for 36h of AZ80-1.0% Nd, respectively.

2.3 Structural characterization

The microstructure and corrosion morphology of the as-cast and heat-treated AZ80-xNd (x=0, 0.5, and 1.0 wt.%) alloy samples were analyzed by scanning electron microscope (SEM, SU-1500) with energy-dispersive spectrometer (EDS). The phase analysis was performed with X-ray diffraction (XRD, D/max-rB-x X-ray diffractometer). After the mass loss measurement, the corroded samples were photographed, and the macroscopic corrosion morphology was observed.

2.4 Mass loss measurement

The corrosion rate of the alloy was measured by the static mass loss. The AZ80-xNd (x=0, 0.5, and 1.0 wt.%) alloys were cut into Φ 30×7 mm sheet by wire cutting machine. After rough grinding, fine grinding, and polishing, the samples were dipped in an anhydrous ethanol (to ensure no water stain on the surface) and dried. The experiment was carried out in 3.5 wt.% NaCl solution, which was kept in a constant temperature water bath at 25 ± 0.5 °C for 72h, with 3 samples in each group. The ratio of solution volume to alloy sample surface area was 30 mL:1 cm^2. Before the experiment, the sample was cleaned ultrasonically in absolute ethanol, dried, and weighed with analytical balance (the accuracy of analytical balance is 0.0001). After the experiment, the sample was taken out and rinsed with deionized water. The corrosion products on the sample surface was cleaned with chromic acid solution (200 g/L CrO_3 + 10 g/L $AgNO_3$) and then weighed. The average corrosion rate (V) of the alloy was calculated by Eq. (1):

$$V = \left(W_0 - W_1\right)/(S \cdot t) \tag{1}$$

where W_0 is the weight of the sample before immersion, W_1 is the weight of the sample after immersion, S is the surface area of specimen, and t is the immersion time.

2.5 Electrochemical measurement

The electrochemical corrosion behaviors of the AZ80-xNd (x=0, 0.5, and 1.0 wt.%) magnesium alloys in 3.5 wt.% NaCl solution were carried out using a Land CHI660E electrochemical system. It was characterized by both potentiodynamic polarization curve and electrochemical impedance

Table 1 Chemical compositions of experimental alloys (wt.%)

Alloy	Al	Zn	Mn	Nd	Si	Mg
AZ80	8.52	0.41	0.27	-	≤0.01	Bal
AZ80-0.5% Nd	8.52	0.41	0.27	0.5	≤0.01	Bal
AZ80-1.0% Nd	8.52	0.41	0.27	1.0	≤0.01	Bal

spectrum (EIS). The experiment was carried out in a three-electrode system, in which the specimen with an exposed area of 1.1 cm^2 acted as the working electrode, while the graphite electrode and saturated calomel electrode acted as the auxiliary electrode and the reference electrode, respectively. Before the experiment, the open circuit potential was operated for 1800s to make the sample stable in the solution. The scanning rate of polarization curve is 1 mV/s. The frequency range of impedance test was 0.01–100,000 Hz, and the amplitude was 5 mV. The impedance behavior was analyzed by the equivalent circuit and fitted by ZSimpwin software.

3 Results and discussion

3.1 Analysis on microstructures

Figure 1 shows the microstructures of the as-cast AZ80-xNd ($x=0$, 0.5, and 1.0 wt.%) magnesium alloys. It can be seen from Fig. 1a that the microstructure of the as-cast AZ80 alloy is composed of primary α-Mg matrix and reticular β-$Mg_{17}Al_{12}$ phase distributed along the grain boundaries. With the addition of Nd element, the β-$Mg_{17}Al_{12}$ phase changed from coarse reticular structure to fine and discontinuous distribution, and a new phase occurs (Fig. 1b and c). It can be seen from Fig. 1b that the addition of 0.5% Nd not only refines the β-$Mg_{17}Al_{12}$ phase, but also reduces the number of β-$Mg_{17}Al_{12}$ phases, which is consistent with other results [18]. Moreover, many studies have shown that the as-cast microstructure of magnesium alloy can be obviously refined by adding appropriate amount of rare earth elements to Mg–Al-Zn alloy, which is mainly due to the formed Al-RE binary phase in the alloy [21]. However, with the increase of Nd content, the grain size of the alloy increases [22, 23]. These results show that proper amount of rare earth Nd can refine the microstructure of the alloy and improve the distribution of β-$Mg_{17}Al_{12}$ phase.

The SEM images of AZ80-xNd ($x=0$, 0.5, and 1.0 wt.%) magnesium alloys in both as-cast and as-solution treated are shown in Fig. 2. It can be seen that there are many rod-shaped and block-shaped phases in the α-Mg matrix after the addition of Nd element to AZ80 alloy, and they increase with the increase of Nd content, as shown in Fig. 2c and e. This indicates that the addition of Nd element leads to the formation of new phases. The main reason is that the electronegativity difference between Mg and Nd is less than that between Al and Nd, so Nd will preferentially combine with Al to form Al-Nd compounds, which has been reported in the literature [24]. At the same time, it can be seen that the addition of 0.5% Nd not only refines the β-$Mg_{17}Al_{12}$ phase, but also reduces the number of β-$Mg_{17}Al_{12}$ phase.

After solution treatment, it is found that the β-$Mg_{17}Al_{12}$ phase distributed along the grain boundaries is almost completely dissolved in the α-Mg matrix (Fig. 2b, d and f), and the Al-Nd compounds with high thermal stability are only partially dissolved (Fig. 2d, f). Many studies have shown that the β-$Mg_{17}Al_{12}$ phase plays a dual role in the corrosion process of Al-Zn magnesium alloys. On one hand, it acts as a cathode phase to accelerate the corrosion of the matrix; on the other hand, it acts as a barrier against corrosion [25]. Therefore, the solution treatment reduces the number of second phase, so that the corrosion rate of the as-solution treatment alloy is faster than that of the as-cast alloy.

EDS analysis (Fig. 2e) shows that the discontinuous phase (area A) consists mainly of Al; therefore, it may be Al-rich phase; both the rod-shaped phase (area B) and the block-shaped phase (area C) are mainly composed of Al and Nd. Therefore, it can be inferred that the rod-shaped phase and block-shaped phase are two different Al-Nd rare earth phases, as detailed in the XRD analysis. Wang et al. [26] pointed out that the new block-shaped Al_2Nd phases are observed in the as-cast AZ80 microstructure after adding Nd element. The results indicated that the addition of Nd not only led to the formation of

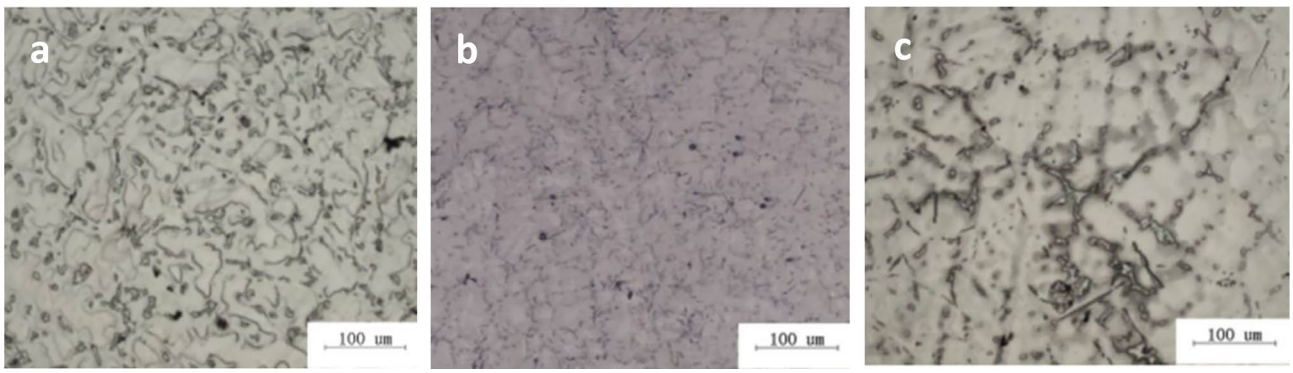

Fig. 1 Optical microscope (OM) images of as-cast samples **a** AZ80; **b** AZ80-0.5% Nd; and **c** AZ80-1.0% Nd

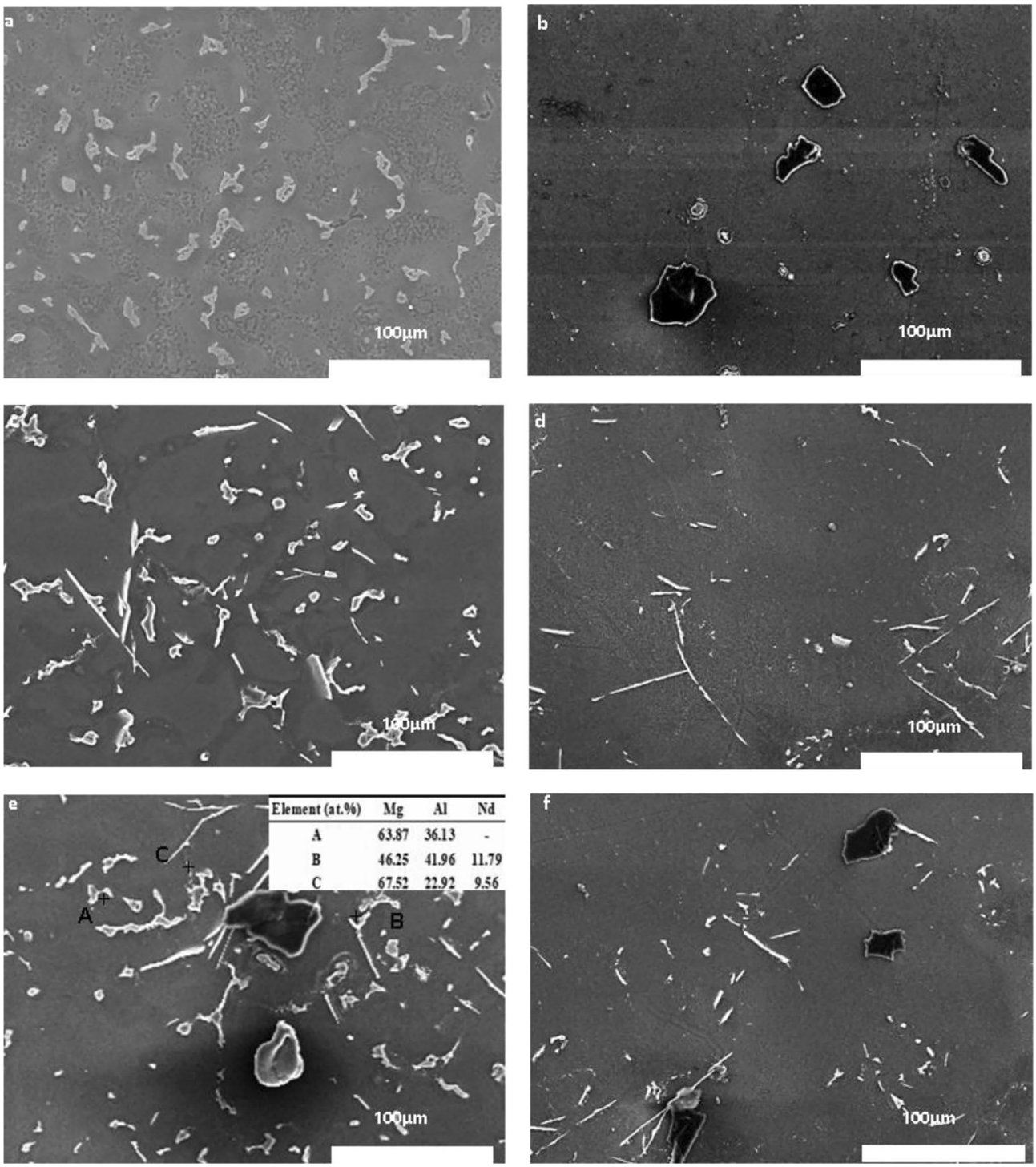

Fig. 2 SEM micrograph of samples **a**,**b** AZ80 F, T4; **c**,**d** AZ80-0.5% Nd F, T4; **e**,**f** AZ80-1.0% Nd F, T4

new phases but also changed the microstructure of AZ80 alloy. Li et al. [27] studied the effects of different contents of rare earth Nd on the as-cast microstructure and corrosion resistance of AZ80 magnesium alloy. It is found that Al_3Nd phase is formed after adding Nd, and the proper amount of Nd can effectively improve the corrosion resistance of AZ80 alloy.

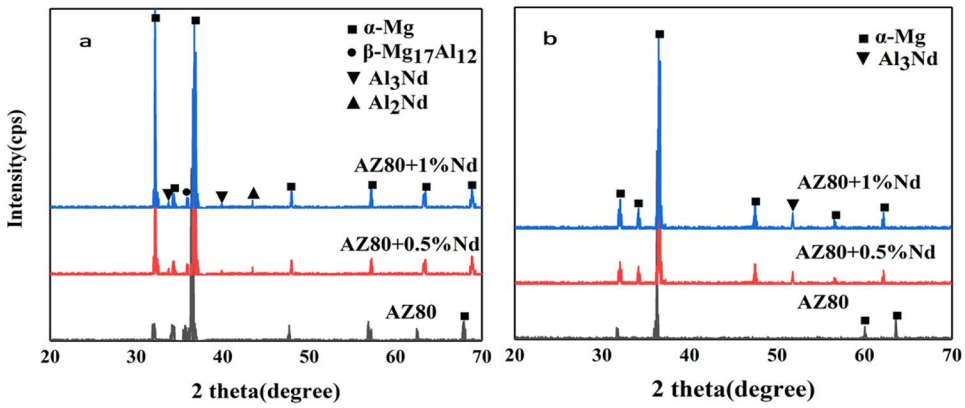

Fig. 3 XRD patterns of AZ80-xNd ($x=0$, 0.5, and 1.0 wt.%) magnesium alloys: **a** as-cast and **b** as-solution treatment

Figure 3 shows the XRD patterns of as-cast and as-solution treated AZ80-xNd ($x=0$, 0.5, and 1.0 wt.%) magnesium alloys, respectively. The as-cast AZ80 magnesium alloy consisted of the α-Mg and β-$Mg_{17}Al_{12}$ phases. With the addition of Nd, an additional peak corresponding to the formation of the Al_3Nd and Al_2Nd phases appeared in the XRD patterns of AZ80-Nd alloy (Fig. 3a). When the Nd content was increased from 0.5 to 1.0 wt.%, the peak intensity of both Al_3Nd and Al_2Nd phases was slightly increased, which indicates that the number of Al-Nd binary phase increases with the increase in the Nd content.

After solution treatment (Fig. 3b), the β-$Mg_{17}Al_{12}$ phase can hardly be detected. This indicates that the β phase is completely dissolved in the α-Mg matrix. This is consistent with the previous microstructural analysis. In addition, from the X-ray diffraction analysis results of the as-solution treated AZ80-Nd alloy, it can be seen that the Al_3Nd phase keeps its diffraction peaks, while the Al_2Nd phase is not detected. This is due to the limited amount of Nd element added and the partial solid solubility of Al-Nd compounds in the magnesium matrix.

The hardness of AZ80-xNd ($x=0$, 0.5, and 1.0 wt.%) magnesium alloys change with time at 175 ℃ is shown in Fig. 4. It can be seen that with the increase in aging time, the hardness of the alloy first increases to the peak and then enters the over aging stage, and the hardness value decreases. The main reason is the diffusion of aluminum atoms towards the grain boundaries to form β-$Mg_{17}Al_{12}$ precipitate. This indicates that precipitation of β-$Mg_{17}Al_{12}$ phase from supersaturated α-Mg solid solution increases continuously with the aging treatment. In addition, studies have shown that the β-$Mg_{17}Al_{12}$ phase precipitates from the supersaturated α-Mg solid solution in two forms:

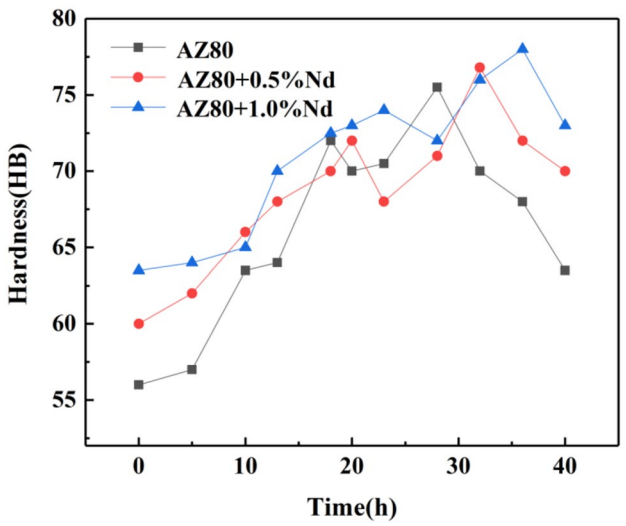

Fig. 4 Hardness of AZ80-xNd ($x=0$, 0.5, and 1.0 wt.%) magnesium alloys aged at 175 °C

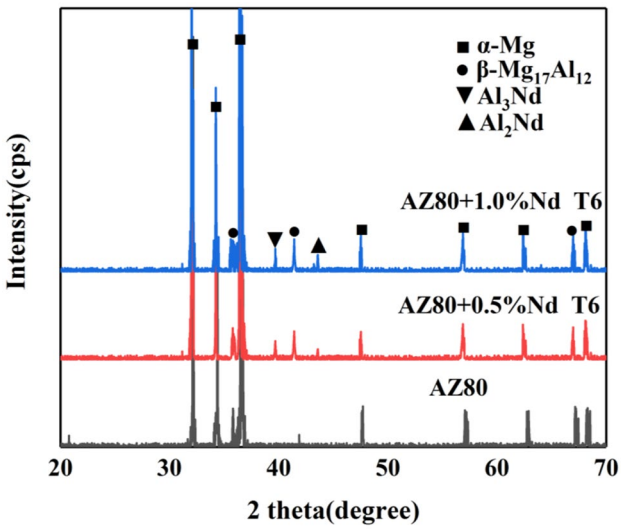

Fig. 5 XRD patterns of AZ80-xNd ($x=0$, 0.5, and 1.0 wt.%) magnesium alloys after aging treatment

discontinuous precipitation and continuous precipitation. With the extension of aging time, discontinuous precipitation stops, and continuous precipitation continues to increase [28]. Clark et al. [29] reported that aging treatment after solid solution will cause the β-$Mg_{17}Al_{12}$ phase previously dissolved in the matrix to precipitate again. Moreover, during aging treatment, the number of β-$Mg_{17}Al_{12}$ phases increases and becomes uniform and fine. In conclusion, with the increase of aging time, β-$Mg_{17}Al_{12}$ phase increases continuously and becomes finer and distributed more uniformly. It can effectively pin the movement of dislocation and increase the dislocation resistance. It plays the role of second phase strengthening and dispersion strengthening, resulting in the obvious increase of the hardness of AZ80-xNd ($x = 0$, 0.5, and 1.0 wt.%) magnesium alloys. Entering the over aging stage, as the β-$Mg_{17}Al_{12}$ phase continues to precipitate and gradually becomes coarser, the hardness of the alloy decreases, which is consistent with the results of Zhao and Kim et al. [30, 31]. In addition, it can be observed from Fig. 4 that the hardness of AZ80-xNd ($x = 0$, 0.5, and 1.0 wt.%) magnesium alloys reach the peak at 28h (75.8 HB), 32h (76.7 HB), and 36h (78 HB), respectively. Moreover, the peak hardness of the alloy increases with the addition of rare earth Nd. The Nd element added to AZ80 alloy promotes the formation of Al_2Nd and Al_3Nd phases. After aging treatment, Nd- phase is dispersed in the alloy as the second phase strengthening agent. The newly formed rare earth phase particles will cause lattice distortion, resulting in a large number of dislocations. Therefore, the hardness of the alloy increases. However, after peak aging, the second phase formed in the alloy gradually coarsens with the increase of the number, which makes the structure of the alloy become uneven and the hardness of the alloy decreased.

The XRD patterns of AZ80-xNd ($x = 0$, 0.5, and 1.0 wt.%) magnesium alloys after aging at 175 °C are shown in Fig. 5. It can be found that the precipitated phase of aged AZ80 alloy is β-$Mg_{17}Al_{12}$ phase, and the Al_3Nd and Al_2Nd are detected with the addition of Nd. The results show that the β-$Mg_{17}Al_{12}$ phase and Al_3Nd and Al_2Nd phases precipitate again after aging treatment.

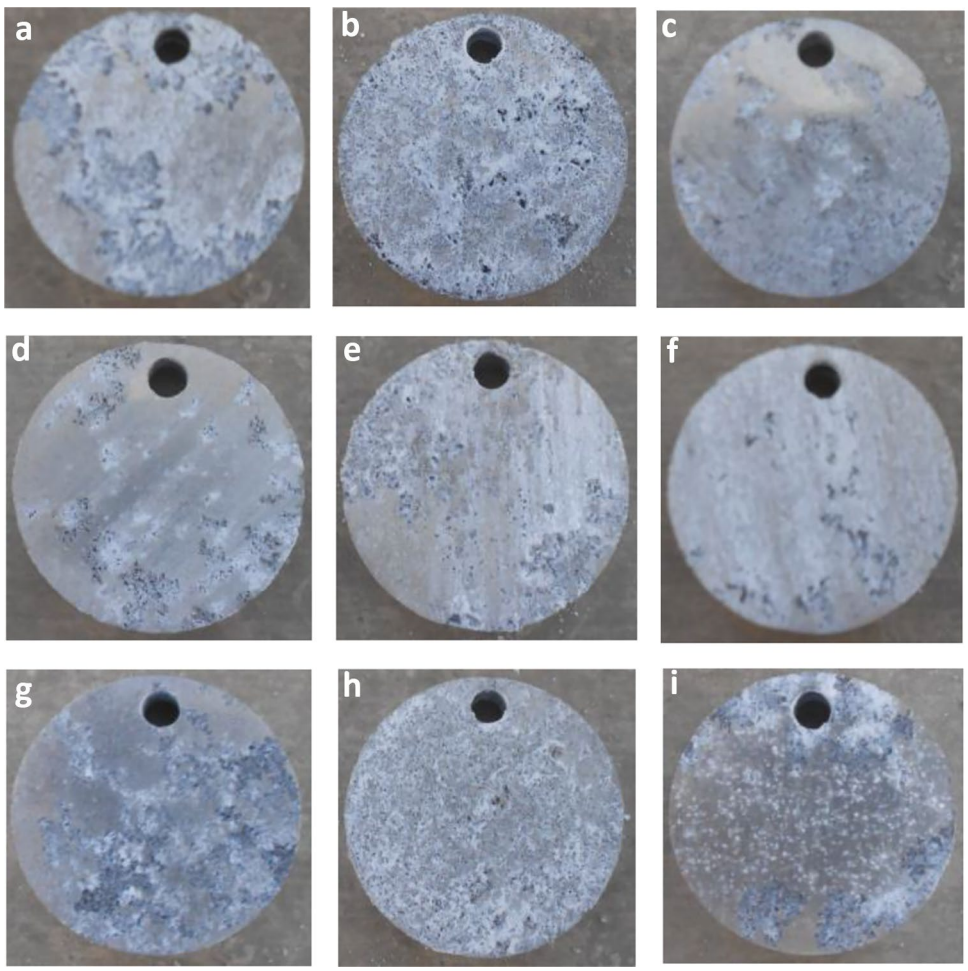

Fig. 6 Macro-pictures of sample after immersion in 3.5 wt.% NaCl solution: **a**,**b**,**c** F, T4, and T6 of AZ80, **d**,**e**,**f** F, T4, and T6 of AZ80-0.5%Nd, **g**,**h**,**i** F, T4 and T6 of AZ80-1.0%Nd

3.2 Analysis on corrosion morphology and corrosion products

3.2.1 Macro-morphology

Figure 6 shows the macro-morphologies of the as-cast and heat-treated AZ80-xNd ($x = 0$, 0.5, and 1.0 wt.%) magnesium alloys immersed in 3.5 wt.% NaCl solution for 3 days. By observing the macro-morphologies of the samples, it is found that the effect of heat treatment on the corrosion behavior of the three alloys with different Nd content is the same. For the as-cast alloy, the alloy surface shows the local corrosion after immersion, and there are many pitting and corrosion pits. For the as-solution treatment alloy, the reticulated β-$Mg_{17}Al_{12}$ phase at the grain boundaries is dissolved in the α-Mg matrix, which reduces the hindrance to the alloy corrosion. Therefore, the as-solution treatment alloy is more prone to corrosion and covered with a large amount of corrosion products. For the aged alloy, the β-$Mg_{17}Al_{12}$ phase and Al-Nd binary phase re-precipitated along the grain boundaries and within the grains, respectively, which slows down the corrosion rate of the alloy.

With the addition of 0.5% Nd, the surface corrosion degree of the as-cast and heat-treated alloys is decreased. Although the pitting also occurs in the localized areas, the corrosion products on the alloy surface are decreased, and the corrosion is lighter. However, when the content of Nd rises to 1.0 wt.%, the corrosion resistance of the alloy is decreased. This is due to the gradual coarsening of the microstructure of the alloy with the continuous increase of Nd content. The results show that under different conditions, the corrosion resistance of the same alloy is AZ80-xNd_{T6} > AZ80-xNd_F > AZ80-xNd_{T4}; under the same conditions, the corrosion resistance of different alloys is AZ80-0.5%Nd > AZ80-1.0%Nd > AZ80.

3.2.2 SEM analysis

Figure 7 shows the SEM images of the as-cast and heat-treated AZ80 magnesium alloys after immersion in 3.5 wt.%

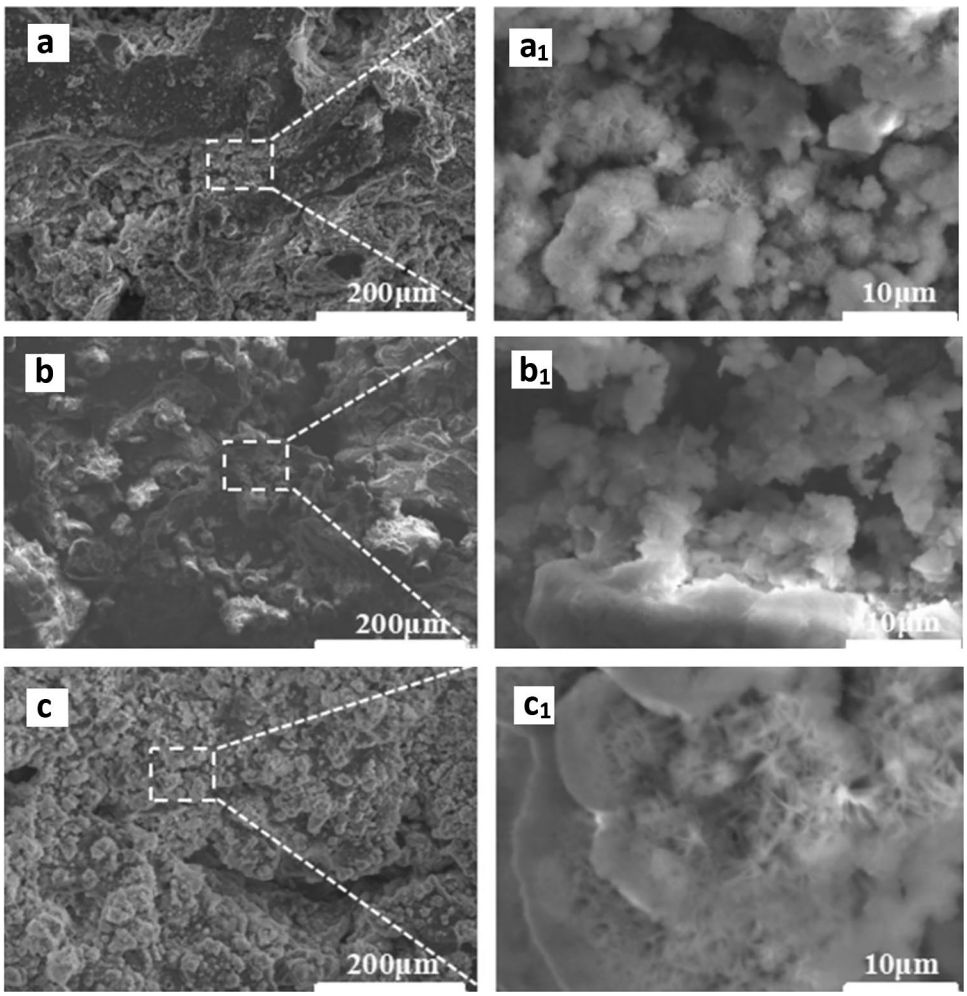

Fig. 7 SEM images of sample after immersion in 3.5 wt.% NaCl solution for 3 days AZ80 (**a**) F, (**b**) T4, (**c**) T6; (right is a local magnification)

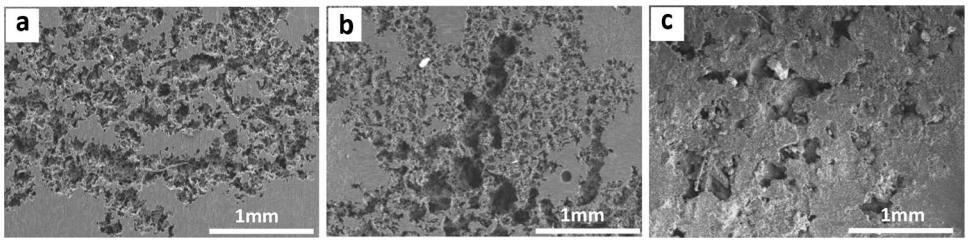

Fig. 8 SEM images of sample after immersion in 3.5 wt.% NaCl solution for 3 days (after cleaning the corrosion products) AZ80 **a** F, **b** T4, **c** T6

NaCl solution for 3 days. Figure 8 shows the SEM image of the as-cast and heat-treated AZ80 alloys after cleaning corrosion products. As shown in Fig. 7a and Fig. 8a, there are corrosion pits on the surface of as-cast AZ80 magnesium alloy, and a large number of corrosion products cover the surface of the alloy. It can be seen from Fig. 7b1 that the corrosion product films formed on the surface of the as-solution treatment alloy is sparse, making it difficult to prevent Cl^- from entering the matrix. Therefore, there are many large and deep corrosion pits on the surface of as-solution treatment AZ80 alloy (Fig. 8b), and finally severe localized corrosion is formed on the surface of the alloy. As can be seen from Fig. 7c1, the corrosion product adheres to the surface of the aged alloy layer by layer, forming a compact corrosion product film, which can effectively restrain the occurrence of corrosion, so the corrosion rate of the aged alloy is decreased. Compared with the as-solution treatment and the as-cast AZ80 alloy, the corrosion of aged AZ80 alloy is the lightest, and the corrosion pits on the surface are the smallest and the least (Fig. 8c).

Figure 9 shows the SEM images of the aged AZ80-0.5%Nd magnesium alloys after immersion in 3.5 wt.% NaCl solution for 3 days. With the addition of 0.5%Nd, there is an obvious corrosion-free area on the aged AZ80-0.5%Nd alloy surface, and the corrosion product is the densest. The addition of Nd leads to the appearance of Nd_2O_3 on the corrosion products of the alloy and forms a dense corrosion product layer on the alloy surface together with magnesium hydroxide. It can effectively restrain the penetration of Cl^- and the occurrence of micro-corrosion on the alloy surface and thereby reduces the corrosion rate of the alloy. This result was also confirmed by Yin, Gu, and Song et al. [32–34].

In summary, AZ80 magnesium alloys with different neodymium contents show pitting after immersion in 3.5 wt.% NaCl solution for 3 days. Moreover, the as-solution treatment AZ80 alloy is corroded most seriously, and the aged AZ80-0.5%Nd alloy is corroded least severely.

3.2.3 XRD analysis

Figure 10 shows the XRD spectra of corrosion products of the aged AZ80-xNd ($x = 0$, 0.5, and 1.0 wt.%) magnesium alloys immersed in 3.5 wt.% NaCl solution for 3 days. From the intensity of the diffraction peaks of the materials, it can be seen that the corrosion products of three alloys mainly consist of α-Mg and $Mg(OH)_2$. In addition, a small amount of $Mg_2(OH)_3Cl{\cdot}H_2O$, MgO and $MgAl_2O_4$ was detected. With the addition of Nd, the MgH_2 and Nd_2O_3 were found in the corrosion products. The formation of MgH_2 reduces the hydrogen evolution, which slows down the cathodic reaction. Thus, the corrosion resistance of the AZ80-Nd alloy is improved.

3.3 Mass loss measurement

Figure 11 shows the average corrosion rate estimated by weight loss tests for the as-cast and heat-treated AZ80-xNd ($x = 0$, 0.5, and 1.0 wt.%) alloys after immersion in a 3.5 wt.% NaCl solution for 3 days. It can be found that

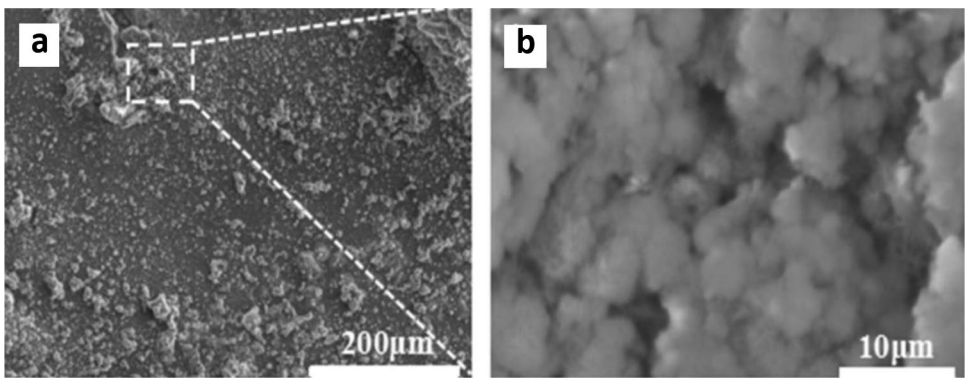

Fig. 9 SEM images of sample after immersion in 3.5 wt.% NaCl solution for 3 days aged AZ80: **a** T6; **b** local magnification

under the same conditions, the corrosion rate of AZ80-Nd alloy is markedly lower than that of AZ80 alloy. However, when the rare earth Nd content is increased to 1.0 wt.%, the corrosion rate of the alloy is slightly higher than that of AZ80-0.5%Nd alloy. The results show that the addition of proper amount of rare earth Nd can improve the corrosion resistance of AZ80-xNd alloy, but too much rare earth Nd will adversely affect the corrosion resistance of the alloy. This remarkable improvement can be attributed to the Al_2Nd and Al_3Nd phases formed within the grain. Because the potential difference between Al-Nd phase and matrix is smaller than that of β-$Mg_{17}Al_{12}$ phase, so the galvanic corrosion in AZ80-Nd alloys is reduced. Especially with the addition of 0.5% Nd, the formation of the Al_2Nd and Al_3Nd phases improves the stability of the passive film on the alloy surface, thus slowing down the corrosion and reducing the corrosion rate of the alloy. The experimental results show that the three alloys have similar corrosion regularities under different heat treatment processes, that is, $V_{T6} < V_F < V_{T4}$. As can be seen from Fig. 11, the as-solution treatment AZ80 alloy has a maximum corrosion rate of 14.12 mg/cm^2/day, and the aged AZ80-0.5%Nd alloy has a minimum corrosion rate of 3.2 mg/cm^2/day.

3.4 Electrochemical measurement

3.4.1 Polarization measurement

Figure 12 shows the polarization curves of as-cast and heat-treated AZ80-xNd (x = 0, 0.5, and 1.0 wt.%) magnesium alloys measured in 3.5 wt.% NaCl, and the fitting results are shown in Table 2. It can be seen that with the addition of Nd, the corrosion potential of AZ80-Nd alloy first increased and then decreased, and the corrosion current density first decreased and then increased. AZ80-0.5%Nd alloy has the maximum corrosion resistance and the minimum corrosion current density under the same conditions, which indicates that its corrosion tendency is low and the corrosion rate is small. This is because the addition of Nd reduces the content of β-$Mg_{17}Al_{12}$ phase and weakens the potential difference between the second phase and matrix. Therefore, the micro-galvanic corrosion of AZ80-xNd (x = 0, 0.5, and 1.0 wt.%) alloys is weakened, so that the corrosion rate of the alloy is decreased. Meanwhile, it can be seen from Table 2 that the aged AZ80-0.5%Nd alloy exhibited a minimum corrosion current density of 5.095×10^{-5} A/cm^2, so the corrosion resistance is the best. This is consistent with the results of weight loss measurement.

3.4.2 EIS measurement

The EIS Nyquist plots of as-cast and heat-treated AZ80-xNd (x = 0, 0.5, and 1.0 wt.%) alloys are depicted in Fig. 13. Two constants can be observed from Fig. 13: a high-frequency capacitive loop and a low-frequency inductance loop, which indicates that pitting may occur. It can be seen that for the same alloy, the capacitor diameter of the as-solution treatment alloy is the smallest and that of the aged alloy is the largest. Moreover, the high-frequency capacitor arc diameter is first increased and then decreased with the addition of Nd element, and the high-frequency capacitor arc diameters of AZ80-0.5%Nd alloy is the largest. Generally speaking, the arc size observed in the impedance spectrum shows the corrosion resistance of the material, and a large arc diameter indicates a high corrosion resistance. Therefore, the

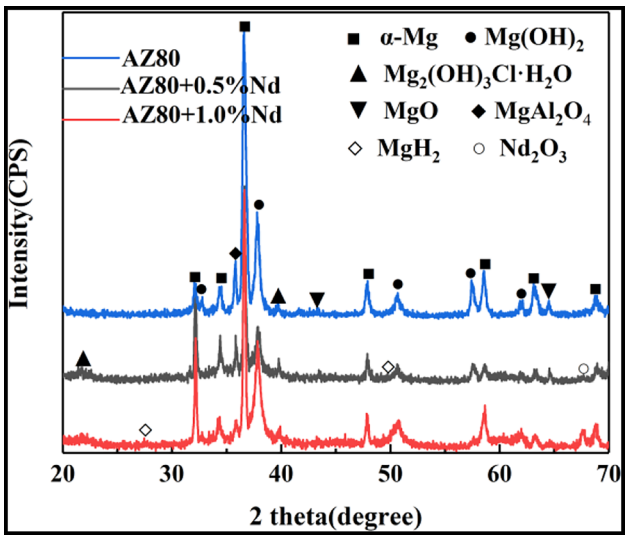

Fig. 10 XRD patterns of corrosion products of the aged AZ80-xNd (x = 0, 0.5, and 1.0 wt.%) magnesium alloys

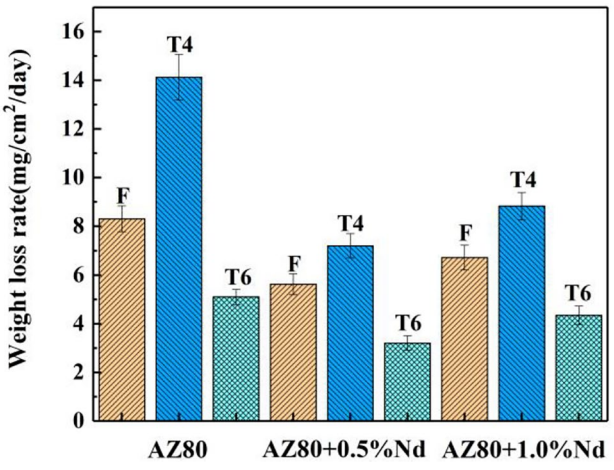

Fig. 11 Average corrosion rates of AZ80-xNd (x = 0, 0.5, and 1.0 wt.%) magnesium alloys estimated by weight loss tests

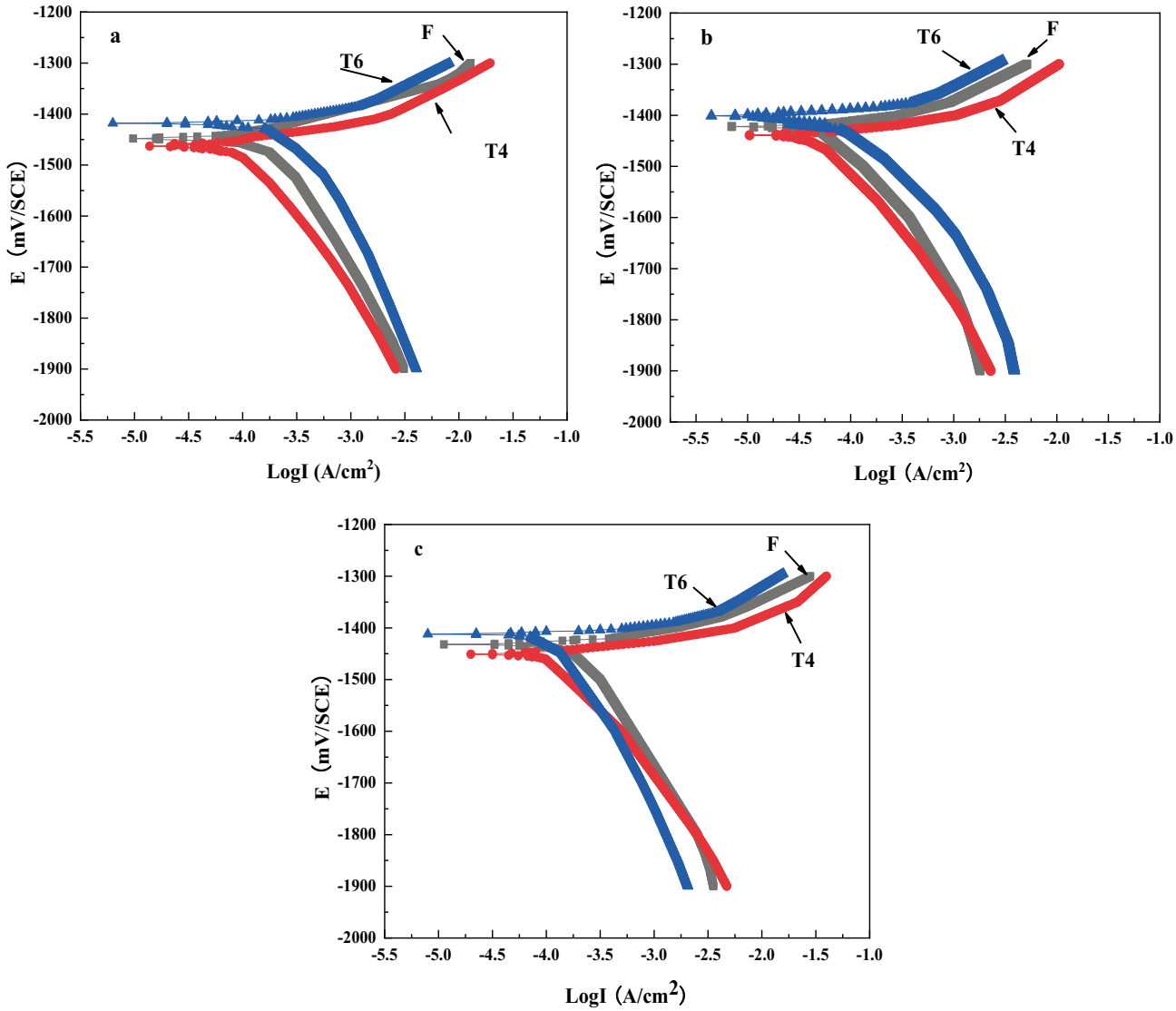

Fig. 12 Polarization curves of as-cast and heat-treated samples in 3.5 wt.% NaCl **a** AZ80; **b** AZ80-0.5% Nd; **c** AZ80-1.0% Nd

corrosion resistance of aging AZ80-0.5%Nd alloy is the highest.

The equivalent circuit and fitting parameters of the studied alloys are shown in Fig. 14 and Table 3, respectively. In this equivalent circuit, R_s is the solution resistance, CPE_{dl} is the double layer capacitance, R_t is the charge transfer resistance, L is inductance, and R_L is the resistance of inductance. It can be seen from Table 3 that for the same condition, the R_t value is first increased and then decreased with the addition of Nd; for the same alloy, the R_t value of the alloy is decreased after solution treatment and increased after aging treatment. Thus, the aged

Table 2 Fitting results of polarization curves of AZ80-xNd (x=0, 0.5, and 1.0 wt.%) alloys

Alloy	F		T4		T6	
Electrochemical parameters	E_{corr}/V	i_{corr}/(A/cm^2)	E_{corr}/V	i_{corr}/(A/cm^2)	E_{corr}/V	i_{corr}/(A/cm^2)
AZ80	−1.446	6.037×10^{-5}	−1.463	6.456×10^{-5}	−1.418	5.347×10^{-5}
AZ80-0.5%Nd	−1.424	5.574×10^{-5}	−1.441	5.896×10^{-5}	−1.398	5.095×10^{-5}
AZ80-1.0%Nd	−1.436	5.713×10^{-5}	−1.453	6.289×10^{-5}	−1.415	5.286×10^{-5}

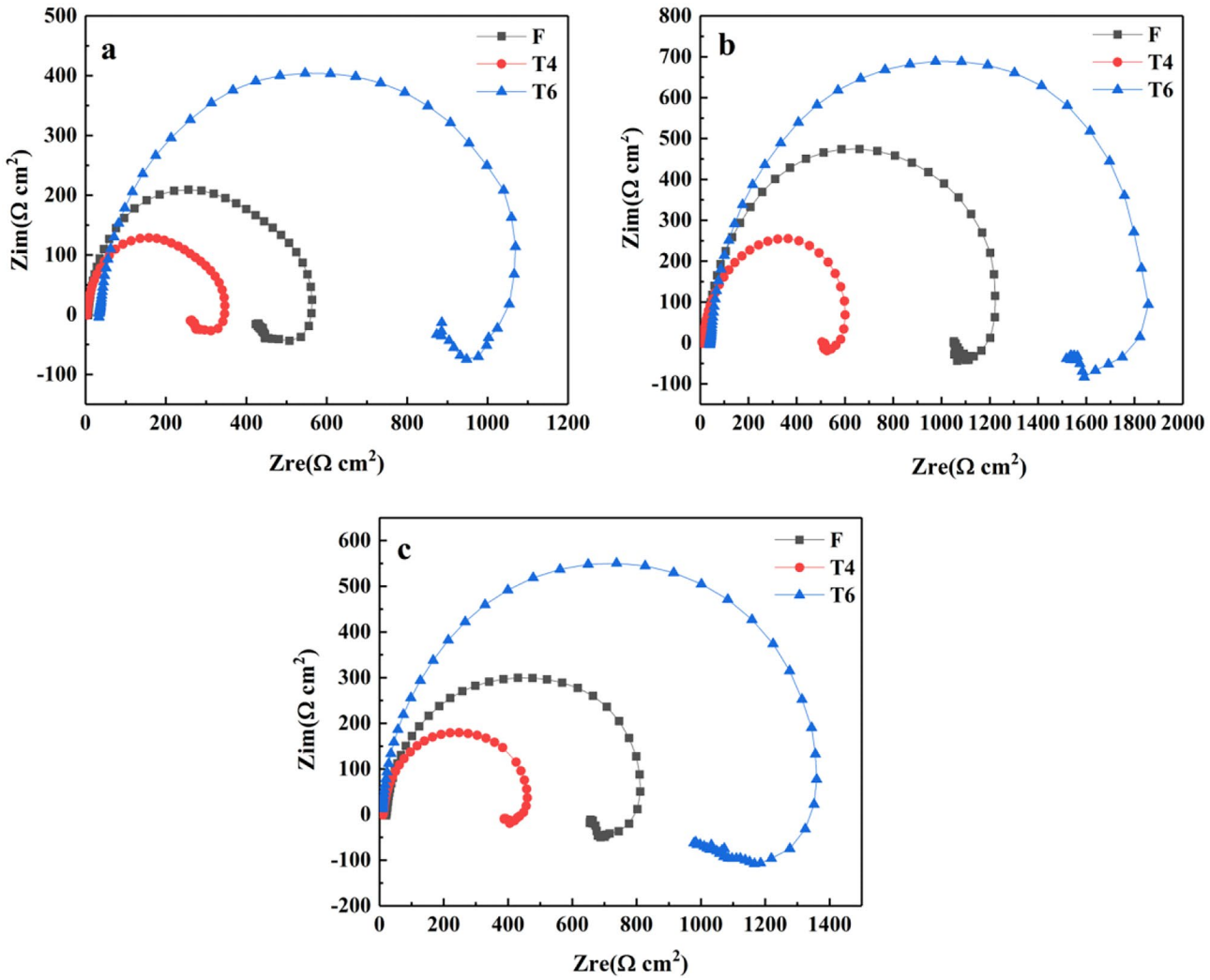

Fig. 13 EIS patterns of as-cast and heat-treated samples in 3.5 wt.% NaCl **a** AZ80; **b** AZ80-0.5%Nd; **c** AZ80-1.0%Nd

AZ80-0.5% Nd alloy has the best corrosion resistance. This is consistent with the results discussed above in mass loss measurement (Fig. 11) and polarization curves measurement (Fig. 12 and Table 2).

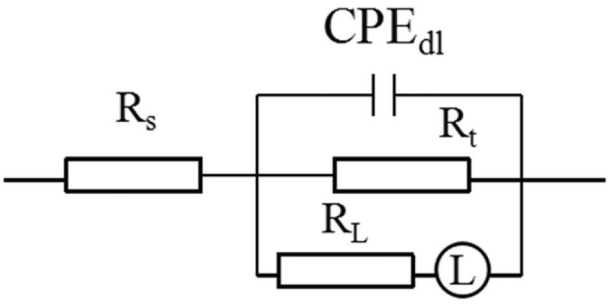

Fig. 14 Equivalent circuit used for fitting the EIS of as-cast and heat-treated AZ80-xNd ($x = 0$, 0.5, and 1.0 wt.%) alloys

4 Corrosion mechanism of alloys

4.1 The effect of second phase on corrosion rates

The corrosion rate of AZ80-xNd ($x = 0$, 0.5, and 1.0 wt.%) alloys is affected by the type, shape, and distribution of the second phase and the potential difference between the second phase and the matrix. From the above analysis, it can be seen that the reticular β-$Mg_{17}Al_{12}$ phase in the as-cast AZ80 magnesium alloy is distributed along the grain boundaries. The results show that it acts as a cathode to form galvanic corrosion with α-Mg matrix, thus accelerating the corrosion rate of the matrix. For the as-cast alloy, after adding 0.5% Nd to the alloy, rare earth Nd is combined with Al to form new rare earth binary phase (rod-shaped Al_3Nd phase and block-shaped Al_2Nd phase), which not only reduces the volume fraction of the β-$Mg_{17}Al_{12}$ phase, but also refines the β-$Mg_{17}Al_{12}$ phase.

Table 3 Fitting parameters obtained from EIS date of as-cast and heat-treated AZ80-xNd ($x=0$, 0.5, and 1.0 wt.%) alloys

Alloy		R_s (Ω cm^2)	CPE_{dl} (Ω^{-1} cm^{-2} S^{-n})	n	R_t (Ω cm^2)
as-cast	AZ80	6.662	9.044×10^{-6}	0.9249	525.5
	AZ80-0.5% Nd	22.58	1.097×10^{-5}	0.8939	1208
	AZ80-1.0% Nd	21.1	1.765×10^{-5}	0.8817	789.8
as-solid solution treatment	AZ80	4.1	1.469×10^{-5}	0.9249	324
	AZ80-0.5% Nd	12.04	2.286×10^{-5}	0.9175	620.2
	AZ80-1.0% Nd	11.64	2.506×10^{-5}	0.8949	452.4
aged	AZ80	33.64	1.056×10^{-5}	0.8838	1046
	AZ80-0.5% Nd	40	7.642×10^{-6}	0.8855	1797
	AZ80-1.0% Nd	6.883	1.005×10^{-5}	0.9158	1343

This is because the difference of electronegativity between Nd and Al is larger than that of between Al and Mg [18, 24], Nd will preferentially combine with Al to form Al_3Nd and Al_2Nd phases. Moreover, the potential of Al-RE binary phase is more negative than that of β-$Mg_{17}Al_{12}$ phase, so the potential difference between the Al-Nd phase and matrix is less than that between β-$Mg_{17}Al_{12}$ phase and matrix [35]. This reduces the driving force of galvanic corrosion in the alloy, so the corrosion resistance of AZ80-0.5%Nd alloy is improved. However, with the continuous addition of Nd, the content of Al is decreased significantly, and Al depletion or enrichment occurs in the local areas, which greatly reduces the corrosion resistance of AZ80 magnesium alloy [36, 37]. Therefore, the corrosion rates of as-cast AZ80-xNd ($x=0$, 0.5, and 1.0 wt.%) alloys are $V_{0.5Nd} < V_{0Nd} < V_{1Nd}$.

The effect of heat treatment on the corrosion resistance of the alloy is largely determined by its effect on the distribution of the second phase in the alloy. For AZ80 alloy, almost all of the β-$Mg_{17}Al_{12}$ phase is dissolved in the α-Mg matrix after solution treatment, as shown in Fig. 2b. Although the reduction of β-$Mg_{17}Al_{12}$ phase is beneficial to avoid the formation of microbattery [38], the corrosion of magnesium alloy preferentially occurs in the poor aluminum area of α-Mg matrix. At the same time, due to the decrease of β-$Mg_{17}Al_{12}$ phase, the protective effect of the second phase on the matrix is weakened, so that the corrosion rate of AZ80 alloy is increased. It is generally believed that aging treatment leads to the precipitation of β-$Mg_{17}Al_{12}$ phase along the grain boundaries, which is beneficial to improve the corrosion behavior of magnesium alloy. This is because aging treatment cause the precipitation of many fine precipitates and some continuous β-$Mg_{17}Al_{12}$ phases in the supersaturated solid solution of magnesium alloy, which increases the content of Al in α-Mg matrix. Meanwhile, the precipitation of β-$Mg_{17}Al_{12}$ phase forms an effective physical barrier of corrosion, so the corrosion resistance of AZ80 magnesium alloy is improved. For AZ80-Nd alloy, except for β-$Mg_{17}Al_{12}$ phase, the Al-Nd binary phase is also dissolved in the matrix after solution treatment. However, due to the lower solid solubility of Nd in magnesium alloy, Al_3Nd phase still exists in AZ80-Nd alloy after solution treatment, as shown in Figs. 2d–f, and 3b. Therefore, after solution treatment, the corrosion resistance of Nd-containing alloy is better than that of AZ80 alloy. Aging treatment leads to the re-precipitation of β-$Mg_{17}Al_{12}$ phase and Al-Nd binary phase in AZ80-Nd alloy, as shown in Fig. 5. Therefore, it can not only effectively restrain the corrosion of the alloy, but also promote the formation of Al, RE oxide and hydroxide, so the corrosion resistance of the alloy is improved [39, 40].

Given all that, the corrosion rate of the same alloy after different heat treatment is $V_{T6} < V_F < V_{T4}$, and the corrosion rate of the three alloys under the same condition is $V_{0.5Nd} < V_{0Nd} < V_{1Nd}$.

4.2 Corrosion Behavior of AZ80 and AZ80-Nd alloy

Combined with the microstructure, corrosion morphology, and corrosion rate of the as-cast and heat-treated alloys under different conditions, the schematic diagrams of corrosion mechanism are shown in Figs. 15–18 for the AZ80 and AZ80-Nd alloy. According to the change of corrosion rate and corrosion morphology under different immersion time, the corrosion process can be mainly divided into four stages, i.e., stage I (Figs. 15a–18a), initial corrosion; stage II (Figs. 15b–18b), film falling off and corrosion products generates; stage III (Figs. 15c–18c), corrosion extension; and stage IV(Figs. 15d–18d), late stage of corrosion.

The schematic of the corrosion mechanism for the as-cast AZ80 alloy in 3.5 wt.% NaCl solutions is shown in Fig. 15. At the stage I (Fig. 15a), the presence of corrosive Cl^- ions will cause rapid corrosion of matrix and formation of a corrosion product layer of Mg $(OH)_2$ on the surface. With the corrosion going on, the corrosion of alloy enters the stage II (Fig. 15b). Because the $Mg(OH)_2$ corrosion layer is sparse and porous, the matrix will be continuously eroded by Cl^-, which causes the Mg$(OH)_2$ corrosion layer fall off from the matrix surface and corrosion pits appear. Therefore, the corrosion rate of the alloy is gradually increased, and new $Mg(OH)_2$ corrosion products are formed continuously.

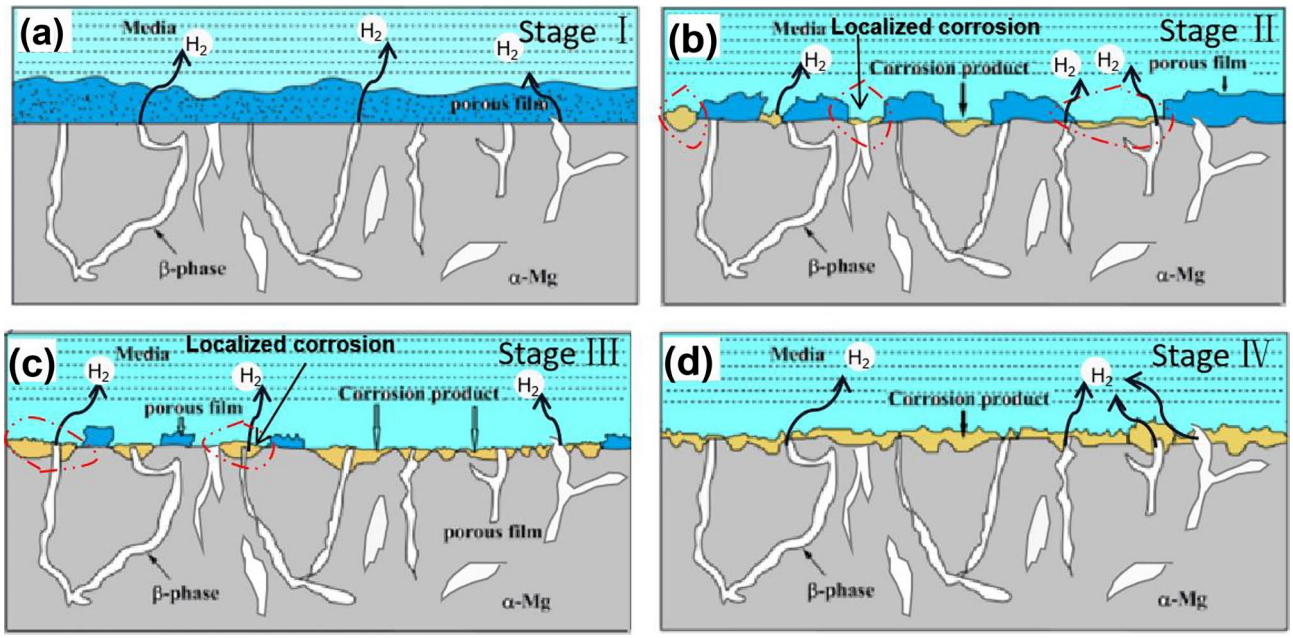

Fig. 15 Schematic of the corrosion mechanism for the as-cast AZ80 alloy in 3.5 wt.% NaCl solution **a** stage I; **b** stage II; **c** stage III; **d** stage IV

In addition, there is a micro-galvanic couple (β-$Mg_{17}Al_{12}$ /α-Mg) at the interface between AZ80 alloy and electrolyte, which leads to a high corrosion rate near the second phase. Thus, the local corrosion mainly occurs near the crude β-$Mg_{17}Al_{12}$ phase, as shown in Fig. 15c (the stage III). As can be seen from Fig. 15d (the stage IV), with the immersion time continuously increasing, the corrosion product layer on the surface of AZ80 alloy gradually is thickened, so that the average corrosion rate of AZ80 alloy gradually is decreased and tends to be stable. Compared with the as-cast AZ80 alloy, the corrosion mechanism of aged AZ80 alloy in 3.5 wt.% NaCl solution is similar to the as-cast AZ80 alloy. However, the main difference between them is that the distribution of the β-$Mg_{17}Al_{12}$ phase is more uniform for

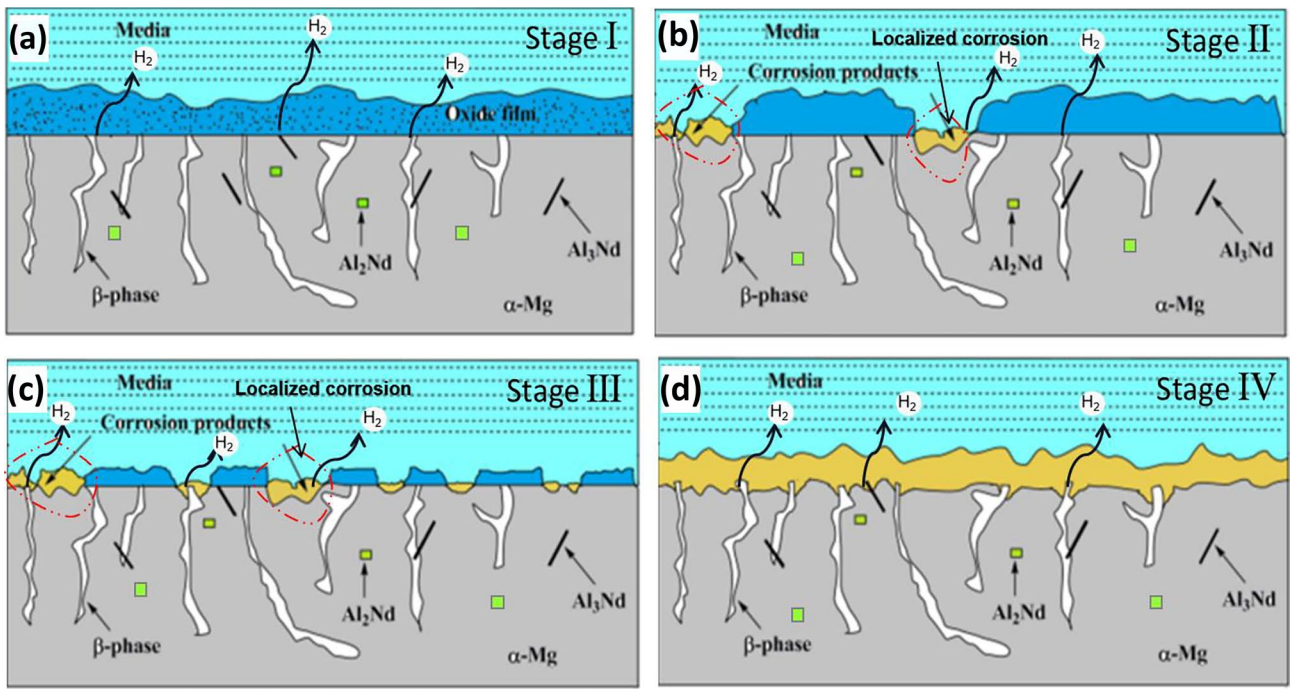

Fig. 16 Schematic of the corrosion mechanism for the as-cast AZ80-Nd alloy in 3.5 wt.% NaCl solution **a** stage I; **b** stage II; **c** stage III; **d** stage IV

the aged AZ80 alloy, forming a continuous corrosion barrier layer. Therefore, the corrosion resistance of aged AZ80 alloy is increased compared with that of as-cast AZ80 alloy.

The schematic of the corrosion mechanism for the as-cast AZ80-Nd alloy in 3.5 wt.% NaCl solution is shown in Fig. 16. It can be seen that with the addition of Nd, the β-$Mg_{17}Al_{12}$ phase becomes finer and more uniform, and the Al_3Nd and Al_2Nd phases are formed. Besides sparse porous Mg $(OH)_2$ film, dense Nd_2O_3 oxide film appears on the surface of AZ80-Nd alloy at the stage I (Fig. 16a). The formation of Nd_2O_3 increases the local positive charge by substituting the magnesium cation. The increased positive charge is assumed to be balanced by trapped anions in the porous magnesium hydroxide layer [41]. Therefore, $Mg(OH)_2$ and Nd_2O_3 corrosion product layers on the surface of AZ80-Nd alloy have dual protection for the matrix and can effectively inhibit the penetration of harmful chloride ions, so as to suppress the further corrosion of the alloy. Moreover, the formation of MgH_2 hinders the occurrence of hydrogen evolution and slows down the process of cathodic reaction; thus the corrosion resistance of the alloy is improved. In the stage II, the film falling off become less with the addition of Nd, and only a small amount of corrosion products appears on the alloy surface. In general, the rare earth binary phase shows active potential. In this experiment, the addition of Nd significantly reduced the proportion of β-$Mg_{17}Al_{12}$ phase and promoted the formation of Al-Nd binary phase with more active potential, which reduces the micro-corrosion caused by its coupling with anode Mg substrate; thus the corrosion rate of AZ80-Nd alloy is reduced. Compared with as-cast AZ80 alloy, AZ80-Nd alloy shows the phenomenon of lighter corrosion and less corrosion pits, as Fig. 16b and c. Finally, as-cast AZ80-Nd alloy presents localized corrosion character (Fig. 16d). Moreover, the corrosion mechanism of the aged AZ80-Nd alloy in 3.5 wt.% NaCl solution is similar to as-cast alloy.

Figure 17 shows the corrosion mechanism of as-solution treatment AZ80 alloy in 3.5 wt.% NaCl solution. As shown in Fig. 17a, almost all of β-$Mg_{17}Al_{12}$ phases in AZ80 alloy dissolved in the matrix. The dissolution of β-$Mg_{17}Al_{12}$ phase reduced the resistance of the second phase to matrix corrosion. Therefore, there are not only a large number of corrosion products accumulated on the surface of the alloy (Fig. 17b), but also corrosion will go deep into the matrix, so many deep corrosion pits are formed (Fig. 17c). In addition, Cl^- in the solution will convert Mg $(OH)_2$ into soluble $MgCl_2$, which makes the magnesium matrix become more active and the effective area of the matrix decreases. As a result, the magnesium matrix is further dissolved, and the surface of the magnesium alloy appears the severe local corrosion (Fig. 17d). Compared with the as-cast AZ80 alloy, the corrosion resistance of the as-solution treatment AZ80 alloy is reduced.

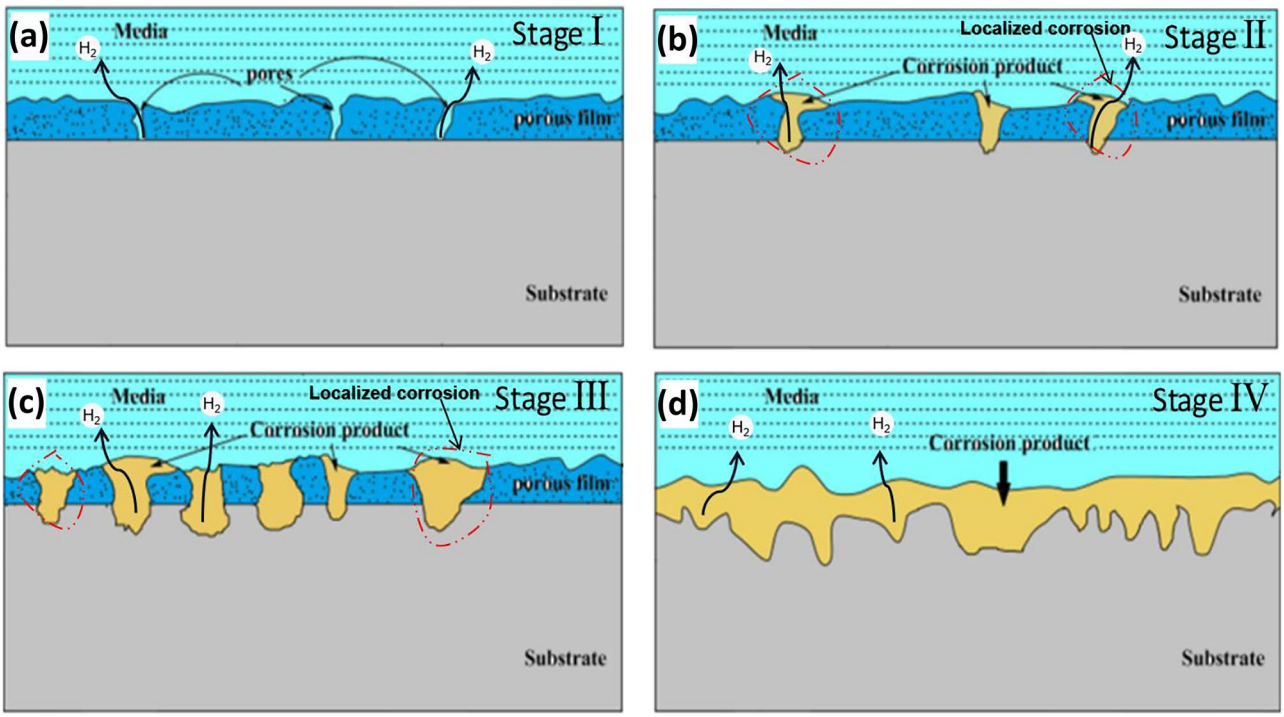

Fig. 17 Schematic of the corrosion mechanism for the as-solution treatment AZ80 alloy in 3.5 wt.% NaCl solution **a** stage I; **b** stage II; **c** stage III; **d** stage IV

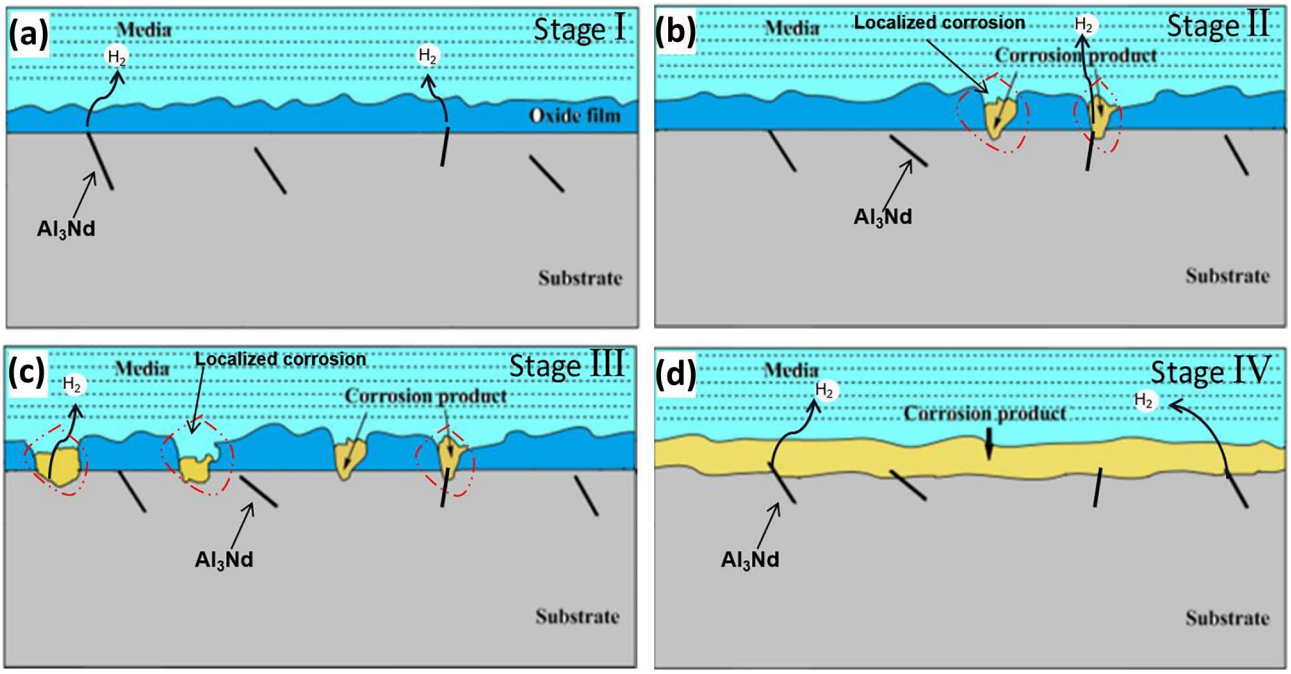

Fig. 18 Schematic of the corrosion mechanism for the as-solution treatment AZ80-Nd alloy in 3.5 wt.% NaCl solution **a** stage I; **b** stage II; **c** stage III; **d** stage IV

Figure 18a–d shows the corrosion mechanism of as-solution treatment AZ80-Nd alloy in 3.5 wt.% NaCl solution. The difference between the as-solution treatment AZ80-Nd alloy and AZ80 alloy is that the Al_3Nd phase is not completely dissolved in the matrix after solution treatment. Therefore, the formed corrosion layers of Mg $(OH)_2$ and Nd_2O_3 on the surface of the alloy can protect the matrix, so the as-solution treatment AZ80-Nd alloy exhibits a slight localized corrosion.

5 Conclusions

1. With the addition of rare earth Nd, new rod-shaped Al_3Nd and block-shaped Al_2Nd phases are formed in the as-cast alloy. This not only restrains the formation of β-$Mg_{17}Al_{12}$ phase, but also transforms β-$Mg_{17}Al_{12}$ phase from coarse reticular structure to fine and discontinuous distribution. Therefore, the corrosion resistance of AZ80-xNd ($x = 0$, 0.5, and 1.0 wt.%) alloy is improved.
2. With 0.5%Nd addition, the grains of the as-cast AZ80 alloy are effectively refined. However, when the content of Nd is 1.0 wt.%, the grain size coarsens remarkably. In addition, with the increase of Nd content, the content of Al-Nd binary phase in the alloy is increased gradually, which increases the galvanic corrosion between the matrix and the second phase, so the corrosion rate of the alloy is increased. As a result, the proper amount of Nd can not only refine the grain structure of the alloy, but also effectively restrain the occurrence of micro-galvanic corrosion, so the corrosion resistance of the alloy is improved.
3. Compared with the aged AZ80 alloy, except for Mg $(OH)_2$, Nd_2O_3 is the new corrosion products existing in the AZ80-Nd alloy. The dense Nd_2O_3 oxide film can more effectively restrain the penetration of Cl^-, so the corrosion rate of the alloy is reduced.
4. After solution treatment, due to the limited content of Nd and the low solubility of Al-Nd binary phase in AZ80-xNd ($x = 0$, 0.5, and 1.0 wt.%) alloy, the Al_3Nd phase is partially dissolved. The results show that solid solution treatment reduces the hindrance of β-$Mg_{17}Al_{12}$ phase and Al-Nd binary phase to matrix corrosion, so that the corrosion rate of as-solution treatment alloy is higher than that of as-cast alloy.
5. After aging treatment, the β-$Mg_{17}Al_{12}$ and Al-Nd binary phase are dissolved in the matrix re-precipitated, and the β-$Mg_{17}Al_{12}$ phase is uniformly and finely distributed in the matrix, so the corrosion resistance of aged alloy is obviously higher than that of the as-cast and as-solution treatment alloys. Finally, AZ80-0.5%Nd alloy shows the best corrosion resistance.

Funding This project was supported by the International Science and Technology Cooperation Program of Shanxi Province (NO: 201603D421024) and the Shanxi Scholarship Council of China (NO. 2017–095, 2019–072).

Declarations

Conflict of interest The authors declare no competing interests.

References

1. Liu W, Cao F, Zhong L, Zheng L, Jia B, Zhang Z, Zhang J (2009) Influence of rare earth element Ce and La addition on corrosion behavior of AZ91 magnesium alloy. Mater Corros 60(10):795–803. https://doi.org/10.1002/maco.200805179
2. Wu F, Zhang S, Tao Z (2011) Corrosion behavior of 3C magnesium alloys in simulated sweat solution. Mater Corros 62(3):234–239. https://doi.org/10.1002/maco.200905510
3. Yang L-j, Wei Y-h, Hou L-f, Zhang D (2010) Corrosion behaviour of die-cast AZ91D magnesium alloy in aqueous sulphate solutions. Corros Sci 52(2):345–351. https://doi.org/10.1016/j.corsci.2009.09.020
4. Candan S, Candan E (2018) Comparative study on corrosion behaviors of Mg-Al-Zn alloys. Trans Nonferrous Met Soc China 28(4):642–650. https://doi.org/10.1016/s1003-6326(18)64696-5
5. Lee JH, Kwak BJ, Kong T, Park SH, Lee T (2019) Improved tensile properties of AZ31 Mg alloy subjected to various caliber-rolling strains. J Magnes Alloy 7(3):381–387. https://doi.org/10.1016/j.jma.2019.06.002
6. Cao H, Huang M, Wang C, Long S, Zha J, You G (2019) Research status and prospects of melt refining and purification technology of magnesium alloys. J Magnes Alloy 7(3):370–380. https://doi.org/10.1016/j.jma.2019.07.002
7. Wu G, Chan KC, Zhu L, Sun L, Lu J (2017) Dual-phase nanostructuring as a route to high-strength magnesium alloys. Nature 545(7652):80–83. https://doi.org/10.1038/nature21691
8. Joost WJ, Krajewski PE (2017) Towards magnesium alloys for high-volume automotive applications. Scr Mater 128:107–112. https://doi.org/10.1016/j.scriptamat.2016.07.035
9. Wang XJ, Xu DK, Wu RZ, Chen XB, Peng QM, Jin L, Xin YC, Zhang ZQ, Liu Y, Chen XH, Chen G, Deng KK, Wang HY (2018) What is going on in magnesium alloys? J Mater Sci Technol 34(2):245–247. https://doi.org/10.1016/j.jmst.2017.07.019
10. Park D-H, Kwon H-H (2015) Development of warm forming parts for automotive body dash panel using AZ31B magnesium alloy sheets. Int J Precis Eng Manuf 16(10):2159–2165. https://doi.org/10.1007/s12541-015-0278-8
11. Zhang X, Dai J, Zhang R, Ba Z, Birbilis N (2019) Corrosion behavior of Mg–3Gd–1Zn–0.4Zr alloy with and without stacking faults. J Magnes Alloy 7(2):240–248. https://doi.org/10.1016/j.jma.2019.02.009
12. Singh IB, Singh M, Das S (2015) A comparative corrosion behavior of Mg, AZ31 and AZ91 alloys in 3.5% NaCl solution. J Magnes Alloy 3(2):142–148. https://doi.org/10.1016/j.jma.2015.02.004
13. Song Y, Shan D, Chen R, Han E-H (2009) Corrosion characterization of Mg–8Li alloy in NaCl solution. Corros Sci 51(5):1087–1094. https://doi.org/10.1016/j.corsci.2009.03.011
14. Zhang J-l, Liu Y-l, Zhou J, Feng Z-y, Wang S-b (2015) Kinetic study on the corrosion behavior of AM60 magnesium alloy with different Nd contents. J Alloy Compd 629:290–296. https://doi.org/10.1016/j.jallcom.2014.12.143
15. Zhang JY, Jia P, Deng YB, Zhao DG, Teng XY (2017) Effect of Nd Addition on the microstructure mechanical and corrosion properties of Mg-Zn-Y-Nd alloys. Mater Sci Forum 898:71–78. https://doi.org/10.4028/www.scientific.net/MSF.898.71
16. Yang M, Liu YH, Liu JA, Song YL (2015) Effect of T6 heat treatment on corrosion resistance and mechanical properties of AM50 magnesium alloy. Mater Res Innov 19(sup10):S10–259-S10–264. https://doi.org/10.1179/1432891715z.0000000002160
17. Zhou W, Shen T, Aung NN (2010) Effect of heat treatment on corrosion behaviour of magnesium alloy AZ91D in simulated body fluid. Corros Sci 52(3):1035–1041. https://doi.org/10.1016/j.corsci.2009.11.030
18. Jiang N, Chen L, Meng L, Fang C, Hao H, Zhang X (2016) Effect of neodymium, gadolinium addition on microstructure and mechanical properties of AZ80 magnesium alloy. J Rare Earths 34(6):632–637. https://doi.org/10.1016/s1002-0721(16)60072-8
19. Zhu Q-F, Wang G-S, Zhang E-G, Liu F-Z, Zhang Z-Q, Cui J-Z (2017) Dynamic and static aging precipitation of β-$Mg_{17}Al_{12}$ in the AZ80 magnesium alloy during multi-directional forging and subsequent aging. Acta Metall Sin Engl Lett 30(10):941–948. https://doi.org/10.1007/s40195-017-0575-6
20. Li H-z, Wei X-y, Ouyang J, Jiang J, Li Y (2013) Hot deformation behavior of extruded AZ80 magnesium alloy. Trans Nonferrous Metals Soc China 23(11):3180–3185. https://doi.org/10.1016/s1003-6326(13)62850-2
21. Xie J-c, Li Q-a, Wang X-q, Li J-h (2008) Microstructure and mechanical properties of AZ81 magnesium alloy with Y and Nd elements. Trans Nonferrous Metals Soc China 18(2):303–308. https://doi.org/10.1016/s1003-6326(08)60053-9
22. Luo TJ, Yang YS, Li YJ, Dong XG (2009) Influence of rare earth Y on the corrosion behavior of as-cast AZ91 alloy. Electrochim Acta 54(26):6433–6437. https://doi.org/10.1016/j.electacta.2009.06.023
23. Zhang A, Hao H, Liu X, Zhang X (2014) Effects of precipitates on grain size and mechanical properties of AZ31-x%Nd magnesium alloy. J Rare Earths 32(5):451–457. https://doi.org/10.1016/s1002-0721(14)60093-4
24. Li MZ, Li C, Liu XG, Liu X, Xu BS (2009) Effect of Nd on microstructure and mechanical properties of AZ31 magnesium alloy. Rare Metal Mater Eng 38(1):0007–0010. https://doi.org/10.1016/S1875-5372(10)60012-4
25. Yin Z, Chen Y, Yan H, Zhou G-h, Wu X-q, Hu Z (2019) Effects of the second phases on corrosion resistance of AZ91-xGd alloys treated with ultrasonic vibration. J Alloys Compd 783:877–885. https://doi.org/10.1016/j.jallcom.2019.01.002
26. Wang Y-x, Fu J-w, Yang Y-s (2012) Effect of Nd addition on microstructures and mechanical properties of AZ80 magnesium alloys. Trans Nonferrous Metals Soc China 22(6):1322–1328. https://doi.org/10.1016/S1003-6326(11)61321-6
27. Li G-l, Wen J-b, He J-g, Ma J-l, Yang Y-s, Li J-f (2013) Effect of Nd addition on microstructure and corrosion resistance of AZ80 magnesium alloys. Trans Mater Heat Treat 34(12):53–58. https://doi.org/10.13289/j.issn.1009-6264.2013.12.009
28. Daud ZC, Azahar SH, Derman MN, Adzali NMS, Zaidi NHA, Adnan SA (2020) The effect of aging time on microstructure and hardness value of AZ80 Mg Alloy. IOP Conf Ser Mater Sci Eng 957(1):012051. https://doi.org/10.1088/1757-899X/957/1/012051
29. Clark JB (1968) Age hardening in a Mg-9 wt.% Al alloy. Acta Metall 16(2):141–152. https://doi.org/10.1016/0001-6160(68)90109-0
30. Zhao D, Wang Z, Zuo M, Geng H (2014) Effects of heat treatment on microstructure and mechanical properties of extruded AZ80 magnesium alloy. Mater Des 56:589–593. https://doi.org/10.1016/j.matdes.2013.11.072
31. Kim SH, Lee JU, Kim YJ (2018) Accelerated precipitation behavior of cast Mg-Al-Zn alloy by grain refinement. J Mate Sci Technol 34(2):265–276. https://doi.org/10.1016/j.jmst.2017.11.019
32. Yin Z, He R, Chen Y, Yin Z, Yan K, Wang K, Yan H, Song H, Yin CX, Guan HY, Luo C, Hu Z, Luc C (2021) Effects of surface micro-galvanic corrosion and corrosive film on the corrosion

resistance of AZ91-xNd alloys. Appl Surf Sci 536:147761. https://doi.org/10.1016/j.apsusc.2020.147761
33. Gu MY, Wei GL, Liu WC, Wu GH (2017) Influence of neodymium on microstructure and corrosion behavior of Mg-8Li-3Al-2Zn alloy. Mater Corros 68:436–443. https://doi.org/10.1002/maco.201609141
34. Song YL, Liu YH, Yu SR, Zhu XY, Wang SH (2007) Effect of neodymium on microstructure and corrosion resistance of AZ91 magnesium alloy. J Mater Sci 42(12):4435–4440. https://doi.org/10.1007/s10853-006-0661-z
35. Mingo B, Arrabal R, Mohedano M, Mendis CL, del Olmo R, Matykina E, Hort N, Merino MC, Pardo A (2017) Corrosion of Mg-9Al alloy with minor alloying elements (Mn Nd Ca Y and Sn). Mater Des 130:48–58. https://doi.org/10.1016/j.matdes.2017.05.048
36. Mathieu S, Rapin C, Steinmetz J, Steinmetz P (2003) A corrosion study of the main constituent phases of AZ91 magnesium alloys. Corros Sci 45(12):2741–2755. https://doi.org/10.1016/s0010-938x(03)00109-4
37. Takenaka T, Ono T, Narazaki Y, Naka Y, Kawakami M (2007) Improvement of corrosion resistance of magnesium metal by rare earth elements. Electrochim Acta 53(1):117–121. https://doi.org/10.1016/j.electacta.2007.03.027
38. Wang BJ, Xu DK, Xin YC, Sheng LY, Han EH (2017) High corrosion resistance and weak corrosion anisotropy of an as-rolled Mg-3Al-1Zn (in wt.%) alloy with strong crystallographic texture. Sci Rep 7(1):16014. https://doi.org/10.1038/s41598-017-16351-z
39. Song G, Atrens A (2003) Understanding magnesium corrosion—a framework for improved alloy performance. Adv Eng Mater 5(12):837–858. https://doi.org/10.1002/adem.200310405
40. Aung N, Zhou W (2002) Effect of heat treatment on corrosion and electrochemical behaviour of AZ91D magnesium alloy. J Appl Electrochem 32:1397–1401. https://doi.org/10.1023/A:1022698916817
41. Yao HB, Li Y, Wee ATS, Pan JS, Chai JW (2001) Correlation between the corrosion behavior and corrosion films formed on the surfaces of Mg82-xNi18Ndx (x=0, 5, 15) amorphous alloys. Appl Surf Sci 173(1–2):54–61. https://doi.org/10.1016/S0169-4332(00)00878-3